SDSS'Rio 2010 STABILITY AND DUCTILITY OF STEEL STRUCTURES
E. Batista, P. Vellasco, L. de Lima (Eds.)
Rio de Janeiro, Brazil, September 8 - 10, 2010

ANALYTICAL DERIVATION OF A GENERALIZED-SLENDERNESS FORMULA FOR IN-PLANE BEAM-COLUMN DESIGN AND COMPARISON WITH INTERACTION-CONCEPT FORMULAE

Andreas Taras*, Richard Greiner*

* Graz University of Technology – Institute for Steel Structures and Shell Structures
e-mails: taras@TUGraz.at, r.greiner@TUGraz.at

Keywords: Beam-Columns, In-Plane Buckling, Interaction Factors, Generalized Slenderness.

Abstract. *This paper presents a new formulation for the design of beam-columns against in-plane buckling that makes use of an -increasingly popular- generalized slenderness definition and an "overall" formulation of the buckling reduction factor for combined load cases. Thereby, great care is placed on accurately describing the specific behavior of each studied cross-sectional type. The result is a "generalized slenderness" formulation that is as accurate, safe and mechanically consistent as the familiar and thoroughly studied interaction-concept formulae.*

1 INTRODUCTION

Beam-columns are characterized by the presence of compressive axial forces N and bending moments M. The resistance of a steel member against either N or M is commonly determined in design codes by the use of buckling reduction factors $\chi = f(\bar{\lambda})$, whereby the plot of the function χ over the normalized slenderness $\bar{\lambda}$ is a so-called buckling curve. The (usually) detrimental effect of the combined action of N and M is taken into account in design codes by formulae that are based on one of the following two concepts, see figure 1:

- The *interaction concept*, found e.g. in clause 6.3.3 of Eurocode 3 [1], makes use of the information contained in the utilizations n_{FB} and m_{LT} of the buckling checks for flexural buckling under N alone and LT-buckling under M alone. The combined effect of N and M is then taken into account by an interaction factor k.

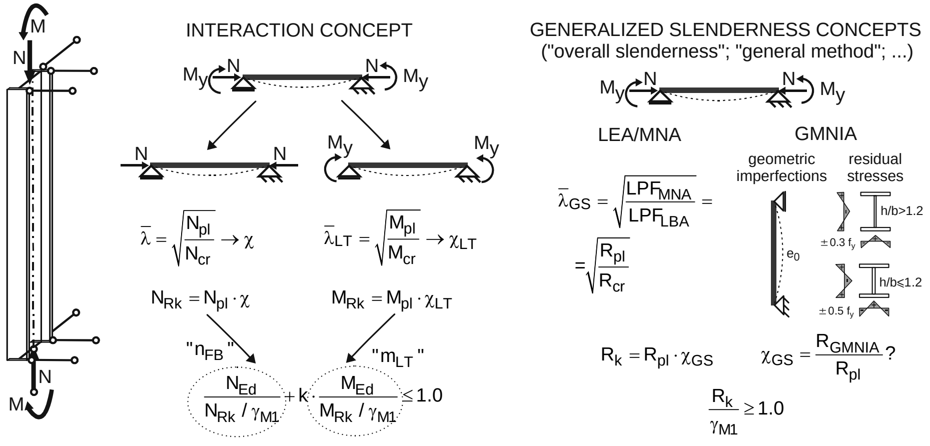

Figure 1: Concepts for beam-column design

- In the second group of concepts, a generalized definition of the (normalized) slenderness is used; they are therefore called *generalized slenderness concepts* in the following. Specifically, these concepts encompass the "overall load case method" used for the design of plates and shells (see e.g. [2]) and the so-called "general method" for the design of beam-columns of clause 6.3.4 in Eurocode 3. These methods have in common that they consider total utilizations for the combined case as basis for the calculation of the normalized slenderness and of the (overall) buckling reduction factor. As is illustrated in figure 1, the slenderness $\bar{\lambda}_{GS}$ is defined in a generalized form as the square root of the total load proportionality factor LPF for the plastic collapse load ($LPF_{MNA}=R_{pl}$) over the pertinent buckling eigenvalue $LPF_{LBA}=R_{cr}$. The buckling strength is then defined as follows:

$$R_{b,d} = \frac{\chi_{GS} \cdot R_{pl}}{\gamma_{M1}} \geq 1.0 \tag{1}$$

Thereby, $R_{b,d}$ is the design buckling resistance (in terms of maximum LPF) of the component or structure against the studied buckling mode for a given load combination.

Even though the current debate over these two concepts might seem to indicate otherwise, the concepts are best thought of as two different forms of representation of the same information, with no basis for attributing an (inexistent) higher degree of mechanical consistency to any of the two. In the case of the interaction concept as found in the Eurocode, mechanical accuracy and safety/reliability have been ensured by extensive theoretical, numerical and statistical studies, summarized in [3]. On the other hand, one could argue that the "generalized slenderness" formulation according to (1) is more "consistent" with the design checks for the single load cases, in the sense that it also implicitly contains the buckling checks used for only N or only M. (In the case of the "general method" this is only true for M, since for N it is based on $\chi_y \cdot N_{pl}$ instead of on N_{pl} alone). However, the reduction factor χ_{GS} must account for the exact same effects as the interaction factor k. As is indicated by the question mark in figure 1, the values to be adopted for χ_{GS} are not clear and still up for debate, with a common opinion being that they must be studied and calibrated by means of GMNIA calculations, see e.g. [4].

The following figure 2 illustrates factors χ_{GS} obtained from such GMNIA calculations for the in-plane buckling behavior of a beam-column under N+M with uniform moment diagram and different values of the ratio $\eta_0=(M/M_{pl})/(N/N_{pl})=m_0/n_0$. Two different definitions of χ and $\bar{\lambda}$ are used. Figure 2a makes use of χ_{ip} and $\bar{\lambda}_{ip}$, which are based on the definitions of R_{pl} and R_{cr} valid for the overall load case N+M and in-plane buckling behavior.

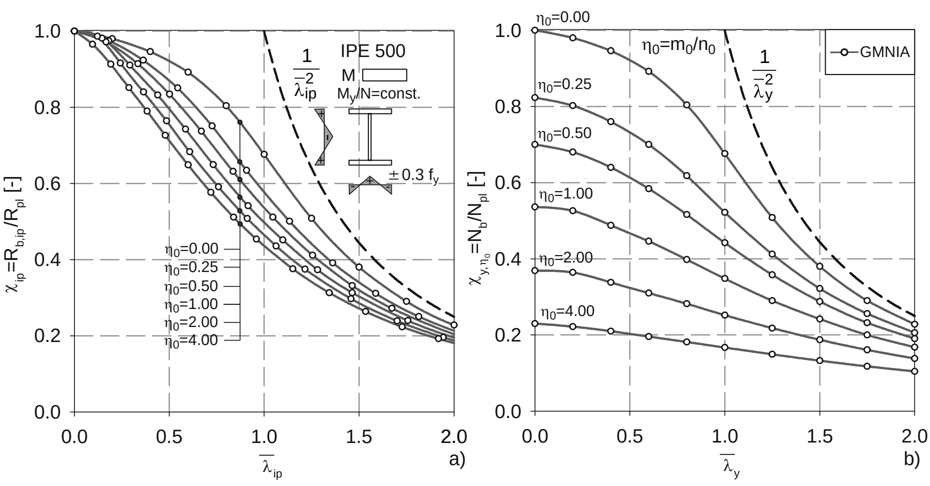

Figure 2: GMNIA buckling reduction factors χ_{ip} (a) and $\chi_{y,\eta 0}$ (b) for in-plane buckling of an IPE 500.

In figure 2b, the familiar definition of the in-plane flexural buckling slenderness $\bar{\lambda}_y$ is used, as well as a representation of the buckling strength for the combined, proportional load case solely in terms of the achievable axial load N_b. Both types of representation yield the same curve for the case of η_0=0.0, representing the (imperfect) column, and result in distinctly different curves for varying values of η_0.

As was mentioned above, any application of a generalized slenderness concept requires a definition/formulation of the buckling reduction factor χ_{GS} that reproduces the same type of information contained in an interaction factor k, thereby achieving high accuracy when compared to more sophisticated GMNIA calculations. This paper presents an analytical formulation for the buckling reduction factors χ_{ip} and $\chi_{y,\eta 0}$ (i.e. χ_{GS} for the in-plane buckling phenomenon of beam-columns) that fulfils this requirement.

2 DEFINITIONS AND ANALYTICAL FORMULATION

This section presents the mentioned proposal for a “generalized slenderness concept” formulation for in-plane beam-column buckling design, focusing on compact class 1 or 2 sections. The full derivation is too lengthy to be included in this paper; thus, the reader is referred to the original source in [5]. However, the basic concepts of the derivation are briefly discussed in the following, making reference to figure 3. The first and essential step of the derivation consists of determining the generalized slenderness for the in-plane buckling case under N+M. Thereby, it is found convenient to do so on the basis of a linearization -with i=1, 2, … linear segments- of the cross-sectional interaction curve, see figure 3a. By introducing the parameters k_{ni} and k_{mi}, the cross-sectional resistance of a section in terms of obtainable values of $m=M/M_{pl}$ and $n=N/N_{pl}$ can be described as follows, for the applicable segment i:

$$k_{ni} \cdot n + k_{mi} \cdot m \leq 1.0 \tag{2}$$

Table 1 contains coefficients k_{ni} and k_{mi} that were derived for a variety of double-symmetric sections. Thereby, the factors η_{SCi} indicate the ratios η=m/n at which the applicable linearized segment of the N/M cross-sectional interaction curve changes; e.g., if $\eta < \eta_{SC1} \longrightarrow k_{ni}=k_{n1}$; $k_{mi}=k_{m1}$.

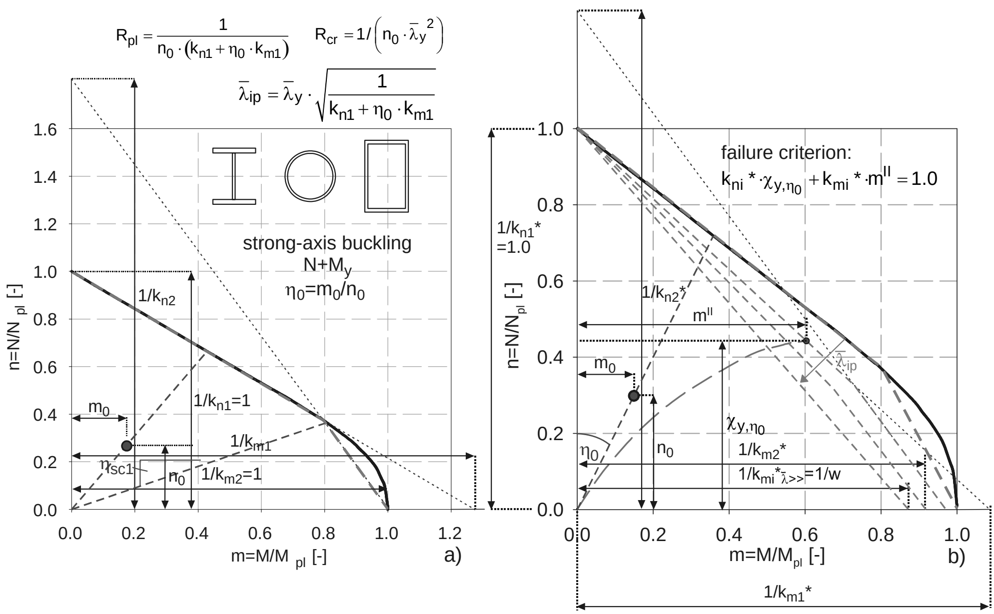

Figure 3: Linearization of the cross-sectional interaction and generalized slenderness definition (a); definition of a second-order failure criterion (b).

Table 1: Ccoefficients used for the description of the cross-sectional N+M interaction behaviour.

#	Type of section, loading, underlying residual stress distributions	Parameters of the N-M interaction linearization	ρ
1	I-section, strong axis buckling $N+M_y$ 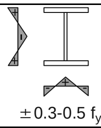	$k_{n1}=1.0;\ k_{m1}=1-0.5\cdot a \geq 0.75\ ;\ \eta_{SC1}=\frac{0.8}{1-0.8\cdot k_{m1}}$	0.8
2	Rectangular hollow section RHS, $N+M_y$ 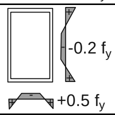	$k_{n2}=\frac{0.2}{1-0.8\cdot k_{m1}}\ ;\ k_{m2}=1.0;\ \eta_{SC2}=\infty$	0.4
3	Circular Hollow Section CHS, N+M 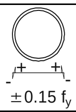	$k_{n1}=1.0\ ;\ k_{m1}=0.74;\ \eta_{SC1}=0.8/(1-0.8\ k_{m1})=1.95$ $k_{n2}=0.2/(1-0.8\ k_{m1})=0.49;\ k_{m2}=1.0;\ \eta_{SC2}=\infty$	0.6
4	I-section, weak axis buckling $N+M_z$ 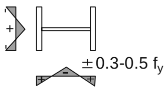	$k_{n1}=1.0;\ k_{m1}=(1-a)/1.45;\ \eta_{SC1}=0.8/(1-0.8\ k_{m1})$ $k_{n2}=0.8/(1.81-a)\ ;\ k_{m2}=(1-a)/(1-0.55a);\ \eta_{SC2}=1/a$ $k_{n3}=0.0;\ k_{m3}=1.0;\ \eta_{SC3}=\infty$	0.6
$a=\frac{A-2\cdot b\cdot t_f}{A}=\frac{A_w}{A}$			

Since the “generalized slenderness” concept operates with load amplification factors R, a reference load level m_0/n_0 is proportionally increased in the following, meaning that the ratio $\eta_0=m_0/n_0=\eta_0$ is kept constant. Taking this into account, the following expressions can be found for the cross-sectional (plastic) amplification factor R_{pl} and the buckling eigenvalue R_{cr} pertaining to the in-plane mode:

$$R_{pl}=\frac{1}{n_0\cdot c_0}=\frac{\eta_0}{m_0\cdot c_0} \tag{3}$$

$$R_{cr}=\frac{1}{n_0\cdot \bar{\lambda}_j^{\,2}} \tag{4}$$

With $c_0=\left(k_{ni}+\eta_0\cdot k_{mi}\right)$; $\bar{\lambda}_j^{\,2}=N_{pl}/N_{cr,j}$; j = axis y or z, depending on the case. The generalized in-plane buckling slenderness can now be written as

$$\bar{\lambda}_{ip}=\bar{\lambda}_j\,/\,\sqrt{c_0} \tag{5}$$

The next step consists of a definition of a (second-order) failure criterion. The basic concept behind the adopted criterion is illustrated in figure 3b: the buckling load of the member is reached when at one cross-section the following condition is fulfilled:

$$k_{ni}*\cdot\frac{N}{N_{pl}}+k_{mi}*\cdot\frac{M^{II}}{M_{pl}}=1.0 \tag{5}$$

Thereby, M^{II} is the total, second-order bending moment in the critical cross-section at failure, while k_{ni}* and k_{mi}* are factors derived –once again- from a linearization of the cross-sectional interaction diagram (see k_{ni} and k_{mi}), but taking into account the transition from the applicability of the plastic and elastic cross-sectional interaction curve with increasing slenderness. This transitional behavior, discussed e.g. in [3] and [5], is caused by the detrimental effect of extreme-fiber (e.g. flange) yielding on the obtainable buckling strength observed in tests or realistic GMNIA calculations. Accordingly, the following expressions (6) and (7) for k_{ni}* and k_{mi}* reproduce a transition from the values k_{ni} and k_{mi} valid for the plastic cross-sectional capacity to the values of $k_{ni}*=1.0$ and $k_{mi}*=W_{pl}/W_{el}=w$ applicable for the elastic cross-sectional resistance at higher slenderness.

$$k_{ni}^* = k_{ni} + (1 - k_{ni}) \cdot \rho \cdot \bar{\lambda}_{ip} \cdot C_{mS} \leq 1 \tag{6}$$

$$k_{mi}^* = k_{mi} + (w - k_{mi}) \cdot \rho \cdot \bar{\lambda}_{ip} \cdot C_{mS} \leq w \tag{7}$$

The factor ρ in (6) and (7) is a numerically calibrated, section-specific value that accounts for the sensitivity to extreme-fiber yielding and is given in table 1 for the different studied types of cross-section. C_{mS} is the equivalent, sinusoidal moment coefficient for in-plane buckling.

For an imperfect beam-column with sinusoidal geometric imperfection of amplitude $\bar{e}_0$ and an in-plane bending moment diagram, the total, second-order bending moment M^{II} in equation (5) can be calculated as follows:

$$M^{II} = \left(C_{mS} \cdot M + N \cdot \bar{e}_0\right) \cdot \frac{1}{1 - N / N_{cr}} \tag{8}$$

The use of (8) in (5) leads to

$$k_{ni}^* \cdot \frac{N}{N_{pl}} + k_{mi}^* \cdot \frac{\left(C_{mS} \cdot M + N \cdot \bar{e}_0\right)}{M_{pl}} \cdot \frac{1}{1 - N / N_{cr}} = 1.0 \tag{9}$$

The next step, explained in detail in [5], consists of replacing the geometric imperfection amplitude $\bar{e}_0$ by the generalized, Ayrton-Perry imperfection amplitude that leads to the EC3 column buckling curves for the studied cross-section and the case where $m_0 = \eta_0 = 0.0$.

$$\bar{e}_0 = \frac{M_{pl}}{N_{pl} \cdot k_{mi}^*} \cdot \eta_{imp} \qquad ; \qquad \eta_{imp} = \alpha \cdot \left(\bar{\lambda} - 0.2\right) \tag{10}$$

The introduction of the normalized terms $\chi_{j,\eta0}=N/N_{pl}$ and $\bar{\lambda}_j = \sqrt{N_{pl} / N_{cr}}$, as well as some simplifying and re-writing, then leads to the following expression:

$$k_{ni}^* \cdot \chi_{j,\eta0} + \left(k_{mi}^* \cdot C_{mS} \cdot \eta_0 + \eta_{imp}\right) \cdot \frac{\chi_{j,\eta0}}{1 - \chi_{j,\eta0} \cdot \bar{\lambda}_j^2} = 1.0 \tag{11}$$

Expression (11) is mathematically equivalent to the Ayrton-Perry type failure criterion used by Maquoi & Rondal [6] to establish and calibrate the well-known column buckling formulae in the Eurocode; this statement is actually only true if the equivalent sinusoidal moment coefficient C_{mS} is expressed independently of the level of the (yet unknown) axial force N at failure. In [5], it is shown how this can be achieved by a very accurate approximation, thereby simply replacing all terms N/N_{cr} in published expressions for C_{mS} by $\bar{\lambda}_j^2/(c_0+\bar{\lambda}_j^2)$. By doing so, (11) can be solved explicitly for $\chi_{j,\eta0}$, leading to the following, familiar-looking expression:

$$\chi_{j,\eta0} = \frac{1}{\Phi_{ip} + \sqrt{\Phi_{ip}^2 - k_{ni}^* \cdot \bar{\lambda}_j^2}} \leq 1.0 \tag{12}$$

with $$\Phi_{ip} = \frac{1}{2} \cdot \left(k_{ni}^* + \eta_{tot} + \bar{\lambda}_j^2\right) \qquad ; \qquad \eta_{tot} = k_{mi}^* \cdot C_{mS} \cdot \eta_0 + \eta_{imp} \tag{13}$$

Expressions (12) and (13) allow for a calculation of buckling reduction factors $\chi_{j,\eta0}$ as exemplified in figure 2b. The "overall", in-plane buckling reduction factor χ_{ip} ,shown in figure 2a, can also be expressed equivalently, as a function of $\bar{\lambda}_{ip}$, by considering (5) and the following relationship:

$$\chi_{ip} = \frac{R_{b,ip}}{R_{pl}} = \frac{\chi_{y,\eta0} / n_o}{1 / \left(n_0 \cdot c_0\right)} = \chi_{y,\eta0} \cdot c_0 \tag{14}$$

This finally leads to the explicit buckling design formula for in-plane beam-column buckling using the "overall" reduction factor χ_{ip}:

$$\chi_{ip} = \frac{c_0}{\Phi_{ip} + \sqrt{\Phi_{ip}^2 - k_{ni}^* \cdot \bar{\lambda}_{ip}^2 \cdot c_0}} \leq 1.0 \tag{15}$$

3 COMPARISON WITH GMNIA RESULTS AND EUROCODE CLAUSES

In this section, the developed expressions (15) and (12) are compared to results of GMNIA calculations, whereby the latter use the common assumptions for geometry and imperfections already used by Beer & Schulz [7] during their elaboration of the numerical & theoretical foundation of the current Eurocode column buckling curves. This ensures consistency with this essential benchmark case.

The first type of comparison is shown in figure 4. In this figure, the evaluations of (15) and (12) are shown in the same type of representation already used for figure 2. Figure 4a shows the “overall” reduction factor χ_{ip}, while figure 4b illustrates the reduction factor $\chi_{y.\eta 0}$ for the obtainable axial load, both for a circular hollow section, proportional loading and different values of η_0. The figure shows that the differences between numerical and analytical curves are very small, and approximately equal for the pure column buckling case (η_0=0.0) and the actual beam-column cases ($\eta_0 \neq$0.0). It can be shown that the type of representation used in figure 4a convergences to a lower-bound curve, while the value of $\chi_{y,\eta 0}$ in fugure 4b of course tends towards zero with increasing values of $\eta_{0.}$ Both phenomena are very well represented by the proposed formulation.

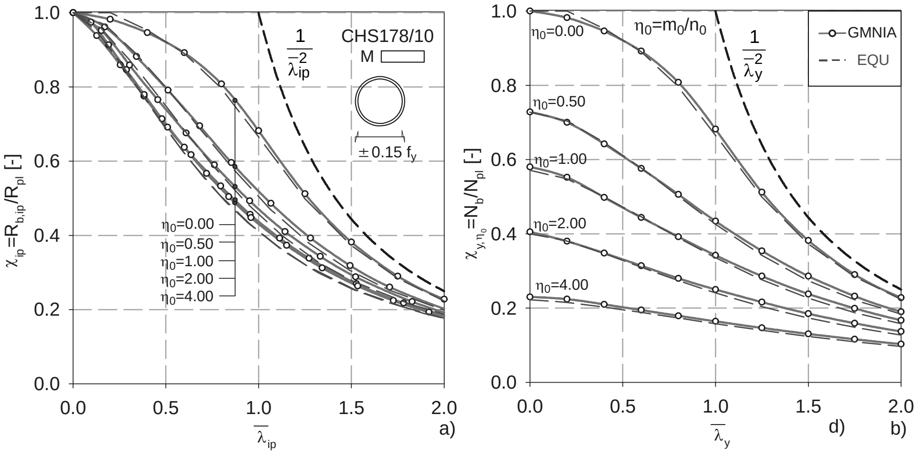

Figure 4: Comparison of newly developed analytical and numerical GMNIA buckling reduction factors χ_{ip} (a) and $\chi_{y,\eta 0}$ (b) for a CHS section.

A different type of comparison is shown in figure 5. In this figure, a spectrum of obtainable combinations of the external loads N+M is plotted for two sections loaded by N + M_y or M_z, whereby three different member lengths and a uniform moment diagram are considered. Figures a) and b) compare the GMNIA results with the current Eurocode “interaction concept” formulae of clause 6.3.3, see [1] and [3]. Figures c) and d) compare the numerical results with the evaluation of the newly developed “overall” expression (15). The accuracy of both the two interaction-concept formulae found in the Eurocode (Annex A and B) and the new formula can generally be said to be excellent.

Some advantages of the new formula can be mentioned here: the fact that expression (15) builds upon an accurate (linearized) description of the actual, section-specific cross-sectional N+M interaction diagram causes it to be “automatically” accurate at very low slenderness, and to lead to a consistent and “correct” transition from the buckling to the (plastic) cross-sectional design check. The latter point is not the case for the two sets of Eurocode interaction factors, which make use of approximations of the cross-sectional interaction for the buckling check and usually don’t lead to the exact interaction at zero slenderness. Another advantage of (15) appears in cases with non-equal end-moments, where failure can be dominated by the cross-sectional check at one of the ends instead of by proper buckling. In the interaction concept, this must be checked specifically, while (15) simply “includes” this check by being limited by 1.0.

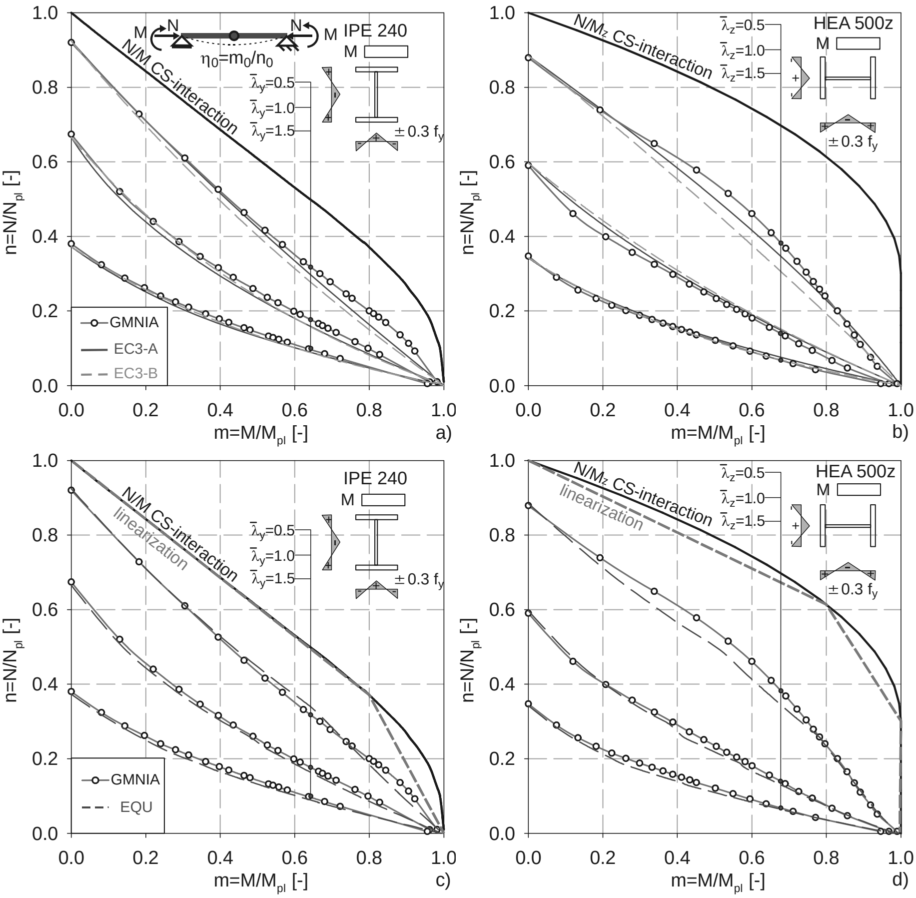

Figure 5: N+M buckling interaction curves according to Annex A & B of Eurocode 3 (a-b) and the analytical formulation (c-d), compared with GMNIA results

In the final figure 6, the numerical GMNIA results, code formulae and the evaluation results of (15) are compared on the level of interaction factors k_j, computed so that they fulfill the following equation:

$$n_j + k_j \frac{M}{M_{pl}} = 1.0 \qquad ; \qquad n_j = \frac{N}{\chi_j \cdot N_{pl}} \tag{16}$$

The top three diagrams in figure 6 compare the values of k_j (k_{yy} or k_{zz}) as defined in Annex A and B of the Eurocode with GMNIA results, while in the bottom three diagrams GMNIA results are compared with (iteratively determined) results of (15) that fulfill (16). Again, the proposed formulation follows the GMNIA values of k_j quite well, especially qualitatively. The curves obtained from (15) appear to have a similar course as the ones of the EC3- Annex A formulae, but with some advantages in accuracy particularly in the case of the circular cross-section, for which the cross-sectional interaction is poorly represented by the Eurocode formulae. It should be noted that the accuracy of the k_j values gives a rather misleading representation of the accuracy of the formulation itself, particularly for higher values of n_y or n_z. Even errors of some 20-30% in terms of k_j only lead to total errors of only a few percentage points at values of n_j beyond 0.5. In this sense, it is a welcome observation that the accuracy of the proposed formulation in terms of k_j is highest for low values of n_j, and mostly conservative in all other cases.

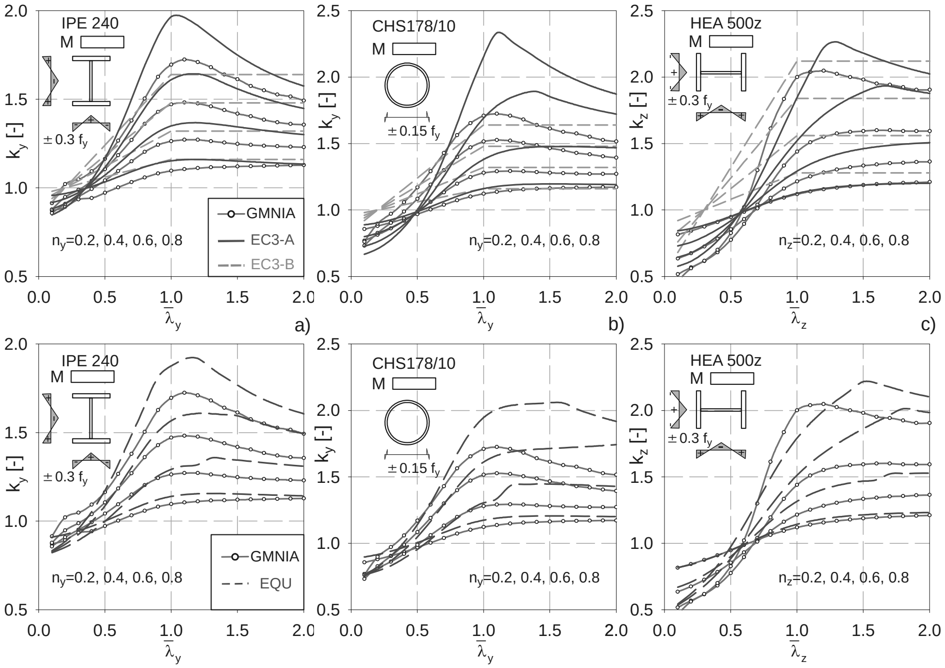

Figure 6: Comparison of interaction factors k_j; top: Eurocode Annex A & B; bottom: new proposal.

4 CONCLUSION

The design proposal in this paper combines the advantages of the “interaction” and “generalized slenderness” concepts for the case of in-plane beam-column buckling. The comparison with numerical results and current Eurocode rules (with many more examples given in [5]) showed the new proposal to have a consistent level of accuracy and safety. The proposal could serve as a procedural blue-print for the expansion of “generalized slenderness” concepts to other member-buckling cases.

REFERENCES

[1] EN 1993-1-1, *Eurocode 3. Design of steel structures. General rules and rules for buildings*, CEN, Brussels, 2005.

[2] Rotter, J.M., *Shell Buckling and Collapse Analysis for Structural Design: The New Framework of the European Standard*, Festschrift for Prof. Calladine, Cambridge, 2002.

[3] Boissonade, N., Greiner, R., Jaspart, J.P., Lindner, J., *Rules for Member Stability in EN 1993-1-1, Background documentation and design guidelines*, ECCS TC 8 – Stability, Brussels, 2006.

[4] Greiner, R., Taras, A., *On the variety of buckling curves*, Proc. of “Stability and Ductility of Steel Structures”, Lisbon (PT), Sept. 6-9, 1101-1108, 2006.

[5] Taras, A., *Contributions to the Development of Consistent Stability Design Rules for Steel Members*, PhD Thesis, Graz University of Technology, 2010.

[6] Rondal, J., Maquoi, R., *Formulations d’Ayrton-Perry pour le Flambement des Barres Métalliques*, Construction Metallique, **4**, 41-53, 1979

[7] Beer, H., Schulz, G., *Bases Théoriques des Courbes Européennes de Flambement*, Construction Métallique, **3**, 37-57, 1970.